Influence of environment on spontaneous emission

Andrii Rudavskyi

Zernike Institute for Advanced Materials, University of Groningen, Nijenborgh 4
9747 AG Groningen, The Netherlands

Spontaneous emission is not a purely intrinsic property of excited system. It very strongly depends on the spectral content of zero-point fluctuations of electromagnetic vacuum, which in its turn is heavily influenced by the presence of boundaries. This article draws attention to the theoretical and experimental aspects of the spontaneous emission rate of excited atoms placed near metallic mirrors, in microcavities and in photonic crystals.

Table of content

1. Introduction

The atomic spontaneous emission rate can be expressed in terms of the zero-point fluctuations of the electromagnetic field at the position of the atom. The local zero-point field fluctuations depend on the photon density of states and on the electromagnetic field strength of the modes. Because the electromagnetic field of the modes depends strongly on the configuration and electromagnetic properties of the material, the spontaneous emission rate can be either increased or decreased, depending on the electric and magnetic properties of the atom's environment.

The possibility of modifying the spontaneous emission rate by changing the environment was first pointed out by Purcell [1] in 1946. Since then, experimental verifications under various conditions have been published. When free atoms are placed inside a cavity, the spontaneous emission rate has been demonstrated to differ from the value in free space [2, 3]. This has also been verified experimentally for certain condensed phase systems inside a cavity [4, 5]. Snoeks *et al.* [6] measured the radiative transition rate at 1.54 µm of erbium ions implanted in a thick glass layer covered by a range of transparent liquids. In [7] Yablonovitch *et al.* studied the spontaneous emission due to the recombination of electron-hole pairs in the more complicated configuration of a GaAs slab bounded by two dielectrics of lower refractive indices. Also Yablonovitch theoretically studied spontaneous emission of atoms imbedded in a so called 'photonic crystal' (PC), which is a dielectric with a dielectric function which is periodic in space. He predicted the appearance of forbidden bands for light in such crystals that would dramatically influence spontaneous emission [8].

Control of spontaneous emission has immediate applications in improving efficiency in semiconductor devices like lasers, diodes, and solar cells [8], and possibly to new technologies like low-threshold lasers, ultrafast optical switchers, all-optical transistors, and memory devices [9].

The aim of this paper is to provide an overview of the work, both theoretical and experimental, and to give a clear idea of how the external environment influences spontaneous emission. That is why we will consider as an external environment different systems starting from the simplest to the more complicated. In the second part of this paper we will present basic quantum mechanical ideas about atomic level transitions and how they can be applied to spontaneous emission in vacuum. In the third part we will consider fluorescence near a mirror. In part 4, the spontaneous emission rate in microcavities will be overviewed. And in the closing part 5, we will consider the theoretical aspects of spontaneous emission in PC.

2. General theory of spontaneous emission

2.1. Spontaneous emission and the Einstein A-coefficient

A free atom or molecule in an excited state does not remain excited but decays to the ground state with a definite lifetime; this decay happens due to radiation which in quantum mechanics is equivalent to unit increase of the occupation number of the electromagnetic field mode.

Spontaneous emission is an interesting phenomenon, which is completely differently treated in different approaches. In semi-classical approach atoms or molecules are considered to be quantum systems with stationary states. According to quantum mechanics if there is no external field such systems remain is corresponding energy levels forever. But in reality transitions occur between levels. Thus in semi-classical theory spontaneous emission decay is introduced phenomenologically by Einstein A-coefficient. The term 'spontaneous emission' originates in that theory and reflects that early idea that the transition occurs by itself, no matter what causes it. As a matter of fact, spontaneous emission is indeed caused by interaction with electromagnetic field, but in this case with so called zero point fluctuations of electromagnetic field. Therefore in correct quantum electrodynamical treatment of this problem, 'spontaneous emission' may be considered as a particular case of stimulated emission. But before calculating spontaneous emission from quantum electrodynamical point of view let us recall derivation of the relation between Einstein's coefficients based on statistical arguments.

Let N_1 and N_2 be a number of molecules in the states of energies E_1 and E_2 correspondingly. According to Boltzmann's law in the equilibrium state they obey the relation:

$$\frac{N_1}{N_2} = e^{-h\nu_{12}/kT} \qquad (2.1)$$

where T is a temperature and $\nu_{12} = (E_1 - E_2)/h$.

Downward transitions occur as the result of irradiation (induced emission) as well as spontaneously. The total rate for downward transitions is written

$$N_1(A_{12} + B_{12}\rho(\nu_{12})) \qquad (2.2)$$

The first term is the spontaneous emission, governed by the rate coefficient A_{12}. The second term is the induced emission, proportional to the energy density $\rho(\nu_{12})$ at frequency ν_{12} and governed by Einstein B-coefficient B_{12}.

The rate for the upward transition is

$$N_2 B_{21}\rho(\nu_{12}) \qquad (2.3)$$

and, at the equilibrium, the upward and downward transition rates are equal, thus we obtain the expression for the energy density distribution function

$$\rho(\nu_{12}) = \frac{A_{12}/B_{12}}{e^{h\nu_{12}/kT}-1} \qquad (2.4)$$

where we used $B_{12} = B_{21}$. If we compare (2.4) with the Planck's law, which was derived from different considerations and describe a spectral content of black body radiation:

$$\rho(\nu_{12}) = \frac{8\pi h\nu_{12}^3}{c^3}\frac{1}{e^{h\nu_{12}/kT}-1} \qquad (2.5)$$

we obtain a relation between Einstein coefficients:

$$A_{12} = \frac{8\pi h\nu_{12}^3}{c^3}B_{12} = \frac{2\hbar\omega^3}{\pi c^3}B_{12} \qquad (2.6)$$

As we can see from (2.6) spontaneous emission rate is completely defined by stimulated emission. Thus even from this statistical approach it is obvious that spontaneous emission depends on the ability of the atom to interact with electromagnetic field.

2.2. A discrete state coupled to the continuum. The Fermi Golden Rule

In many optical processes, including absorption and emission of light, transitions take place between levels one or both of which lie within a continuous spectrum. In absorption the initial state is the molecule's ground state plus n-quanta of radiation field, the excited modes of which span a continuous range of frequencies near the resonant frequency of the molecular transition. The final state is the combination of the excited molecule and (n-1)-quanta of the radiation field. In spontaneous emission the initial state is discrete (excited molecule plus vacuum field) and the final state continuous (for example light can be emitted in all directions). To be able to calculate spontaneous emission rate we first have to learn how to calculate transition probability from discrete state to continuous band.

We can imagine continuous band as a set of discrete levels within frequency range $\Delta\omega$ which are situated very closely to each other. Suppose system is in the initial state $|i\rangle$ and it transfers into a continuous band that is a set of final states $|f\rangle$. To find a probability of such transition we have to sum transition probabilities for each level using well known formula:

$$P_{total}(t) = \sum_f P_{fi}(t) = 4\sum_f \frac{\left|\langle f|V|i\rangle\right|^2}{\hbar^2}\frac{\sin^2 \omega_{fi}(t-t_0)/2}{\omega_{fi}^2} \qquad (2.7)$$

where V is transition operator and $\langle f|V|i\rangle$ is a matrix element of the transition, $(t-t_0)$ time of interaction with electromagnetic field and summation is over all levels of the energy band. To accomplish this summation we use the fact that the separation between levels is very small; then we can introduce the density of states defined as number of states per unit energy. Then the sum over $|f\rangle$ is replaced by integral:

$$P_{total}(t) = \frac{4}{\hbar}\int_{\omega_i-\Delta\omega/2}^{\omega_i+\Delta\omega/2}\left|\langle f|V|i\rangle\right|^2 \frac{\sin^2 \omega_{fi}(t-t_0)/2}{\omega_{fi}^2}\rho_f d\omega_f \qquad (2.8)$$

$$= \frac{1}{\hbar}\int_{\omega_i-\Delta\omega/2}^{\omega_i+\Delta\omega/2}\left|\langle f|V|i\rangle\right|^2 F(t,\omega_{fi})\rho_f d\omega_f$$

Although $\left|\langle f|V|i\rangle\right|^2$ and ρ_f are functions of ω_f, they are slowly varying near ω_i compared with $F(t,\omega_{fi})$ and may be treated as constant. Thus (2.8) becomes:

$$P_{total}(t) = \frac{2(t-t_0)}{\hbar}\left|\langle f|V|i\rangle\right|^2 \rho_f \int_{-\Delta\omega(t-t_0)/4}^{\Delta\omega(t-t_0)/4}\frac{\sin^2 y}{y^2}dy$$

$$\xrightarrow{\Delta\omega(t-t_0)\gg 1} \frac{2(t-t_0)}{\hbar}\left|\langle f|V|i\rangle\right|^2 \rho_f \int_{-\infty}^{\infty}\frac{\sin^2 y}{y^2}dy \qquad (2.9)$$

$$= \frac{2\pi}{\hbar}\left|\langle f|V|i\rangle\right|^2 (t-t_0)\rho_f$$

Thus the probability is proportional to the time interval, so that it is possible to define a transition rate:

$$\frac{dP}{dt} = \Gamma = \frac{2\pi}{\hbar}\left|\left\langle f|V|i\right\rangle\right|^2 \rho \qquad (2.10)$$

which is the well-known Fermi Golden Rule.

2.3 Spontaneous emission in vacuum

In quantum electrodynamics excited atom or molecule is a part of a system which also includes radiation field. Excited atom interacts with this field even when it is in its vacuum state, leading to radiative decay. During this decay atom always remain in discrete states but electromagnetic field converts from its vacuum state into continuum band of states. Using technique developed in previous subsection we can calculate the transition probability of the whole system 'atom-electromagnetic field'.

Let the initial state be represented by $\left|E_m;0\right\rangle$, where $\left|E_m\right\rangle$ is the m-th state of the atom or molecule and $\left|0\right\rangle$ refers to the vacuum state of the electromagnetic field. Suppose, after radiation system decayed to the state $\left|E_0;1(\vec{k})\right\rangle$, where $\left|E_0\right\rangle$ is the ground atomic state and $\left|1(\vec{k})\right\rangle$ is a state of emitted photon.

To get the emission probability we first have to calculate the matrix element which is included in formula (2.10):

$$\left\langle f|V|i\right\rangle = \left\langle 1(\vec{k});E_0\left|-\vec{\mu}\cdot\vec{E}(\vec{R})\right|E_m;0\right\rangle$$
$$= -\vec{\mu}^{0m}\cdot\left\langle 1(\vec{k},\lambda)\left|\vec{E}(\vec{R})\right|0\right\rangle \qquad (2.11)$$

After expressing electromagnetic field via its quantum characteristics we obtain an expression for matrix element:

$$\left\langle f|V|i\right\rangle = \left(\frac{\hbar ck}{2\varepsilon_0 V}\right)^{1/2}\mu_i^{0m}e^{-ik\vec{R}} \qquad (2.12)$$

It is convenient in the first instance to calculate the rate of emission into a cone of solid angle $d\Omega$ centered around $\vec{k}$. For this purpose we need an expression for the density of final states. It is easy to show that the number of modes in a volume V with wave vector between $\vec{k}$ and $\vec{k}+d\vec{k}$ is $Vd^3\vec{k}/(2\pi)^3$, which in terms of spherical polar coordinates is $V/(2\pi)^3 k^2 dk d\Omega$. This represents the number of levels with energy between $\hbar ck$ and $\hbar c(k+dk)$ with the wave vector lying within the solid angle $d\Omega$ around direction $\vec{k}$. Thus the density of final states is given by

$$\rho_f = \frac{k^2 d\Omega}{(2\pi)^3 \hbar c}V \qquad (2.12)$$

Using (2.11) and (2.12) in Fermi golden rule, we get

$$d\Gamma(\Omega) = \frac{2\pi}{\hbar}\left(\frac{\hbar ck}{2\varepsilon_0 V}\right)\mu_i^{0m}\bar{\mu}_j^{0m}\frac{k^2 d\Omega}{(2\pi)^3 \hbar c}V \qquad (2.13)$$

Since the molecules are randomly oriented with respect to laboratory frame, an orientation average is required. Thus

$$\left\langle d\Gamma(\Omega)\right\rangle = \frac{2\pi}{\hbar}\left(\frac{\hbar ck}{2\varepsilon_0 V}\right)\frac{\left|\bar{\mu}^{0m}\right|}{3}\frac{k^2 d\Omega}{(2\pi)^3 \hbar c}V \qquad (2.14)$$

In these calculations we implicitly assumed that radiated field has fixed polarization, but each emitted photon has one of two independent polarizations; that gives another factor of 2. After integration over the whole solid angle:

$$\Gamma = \frac{k^3}{3\varepsilon_0\pi\hbar}\left|\bar{\mu}^{0m}\right|^2 = \frac{\omega^3}{3\varepsilon_0\pi\hbar c^3}\left|\bar{\mu}^{0m}\right|^2 \qquad (2.15)$$

This spontaneous emission rate applies to an atom or a molecule in free space. If the system of molecule plus electromagnetic field is contained within a cavity the rate can be radically altered. The new boundary conditions at the walls of the cavity impose changes of the mode structure as well as the level density of the radiation field. The coupling of the atom or molecule to the electromagnetic vacuum is changed as a result. For example, if the transition frequency for emission is less then the fundamental frequency of cavity, spontaneous emission is significantly inhibited. This modification due to space confinement will be considered in the following chapters.

3. Excited molecule near plane mirror

Drexhage [10] carried out the earliest experimental demonstration of SpE rate modification by studying the emission of dye molecules close to a metallic mirror. It was shown that the presence of the mirror in the vicinity of the molecule strongly modifies both spontaneous emission and angular distribution of its fluorescence. The degree of modification depends on the exact distance between molecules and mirror. For large distances (d>20 nm) the SpE rate was found to display oscillatory dependence on the dye-mirror separation. This change is caused by the fact that the phase of retarded molecular dipole fields reflected from the mirror, which drive the dipole, depends on dye-mirror separation. Depending on the phase of these retarded molecular dipole fields it is possible to observe either enhancement or inhibition of the emission (the dipole is driven in or out of phase respectively). For molecules in very close proximity to the metallic mirror (d<20 nm), the strong quenching of the emission was observed. This was found to be largely due to the excitation of surface plasmon-polaritons (SPP) propagating at the metal dielectric interface. This was experimentally proved by Pockrand and Brillante [11] and theoretically studied in works [12, 13]. Classical and quantum electrodynamical models were developed for Drexhage's system in works [14, 15]. An overview of these works is given in this chapter.

3.1 Classical approach

In this approach the system, fluorescing atom-mirror, can be represented as a classical oscillator and its image. Initially the excited atom decays as if it was in free space until it "feels" the mirror after time $t = 2d/c$ (d distance to the mirror). The force acting on the oscillator (charge e, mass m) at a distance x of its equilibrium position is given by the equation of motion $m\ddot{x} = -kx - m\Gamma\dot{x}$. k is the elastic constant and Γ is the friction force constant; $\Gamma = \Gamma_e + \Gamma_n$, where Γ_e and Γ_n is the radiative and non-radiative term respectively ($\tau = 1/\Gamma$ decay time). According to Hertz Γ_e is given by:

$$\Gamma_e = \frac{2}{3}\frac{e^2\omega^2 n}{c^3 m} \qquad (3.1)$$

where c velocity of light, n refractive index of dielectric medium surrounding dipole, $\omega^2 = k/m$.

When the mirror is included the reflected wave F_R form the mirror must also be considered, and the equation $m\ddot{x} = -kx - m\Gamma\dot{x} + F_R$ must hold. This may be rewritten in terms of the dipole moments $\mu = ex$:

$$\ddot{\mu} + \omega^2 \mu = \left(e^2 / m\right) F_R - \Gamma \dot{\mu} \qquad (3.2)$$

F_R is determined by Hertz's field of the oscillator, modified by a phase shift δ at the reflection, and by the reflectivity R^2. Kuhn in [14] has shown that for the case of a dipole oscillating parallel to the surface the expression for the reflected field may be written in the form:

$$F_R = \alpha \mu + \beta \dot{\mu} \qquad (3.3)$$

$$\alpha = \frac{R\omega^3 n}{c^3} \left[\left(-\gamma^{-3} + \gamma^{-1}\right) \cos(\gamma - \delta) - \gamma^{-2} \sin(\gamma - \delta) \right] \qquad (3.4)$$

$$\beta = -\frac{R\omega^2 n}{c^3} \left[\left(-\gamma^{-3} + \gamma^{-1}\right) \sin(\gamma - \delta) + \gamma^{-2} \cos(\gamma - \delta) \right] \qquad (3.5)$$

$$\gamma = \omega \frac{2\pi d}{c} \equiv 4\pi n \frac{d}{\lambda} \qquad (3.6)$$

γ is a phase of reflected field. By inserting (3.4) and (3.5) into (3.3):

$$\ddot{\mu} = -[\omega^2 - \left(e^2 / m\right)\alpha]\mu - [\Gamma - \left(e^2 / m\right)\beta]\dot{\mu} \qquad (3.7)$$

The decay time (τ_d) is the inverse of the damping factor in (3.7). Using (3.5) and (3.6):

$$\frac{\tau}{\tau_d} = 1 + \frac{3}{2} qR \left(-\frac{\sin(\gamma - \delta)}{\gamma^3} + \frac{\sin(\gamma - \delta)}{\gamma} + \frac{\cos(\gamma - \delta)}{\gamma} \right) \qquad (3.8)$$

From (3.4) we can see oscillatory dependence of the excitation lifetime on phase γ, in other words on atom-mirror separation. This dependence is plotted in Fig. 1. and shows good agreement with the experiment.

3.2 Quantum mechanical approach

For quantum mechanical treatment of this problem let us come back to Fermi golden rule and use it in the form equivalent to (2.7):

$$\Gamma = \frac{2\pi}{\hbar^2} \sum_f \left| \left\langle f \left| \vec{\mu} \cdot \hat{\vec{E}}(r_0, t) \right| 0 \right\rangle \right|^2 \delta(\omega_f - \omega_0) \qquad (3.9)$$

The electric field operator can be written in the form of:

$$\hat{\vec{E}}(\vec{r}, t) = \frac{1}{\sqrt{2\pi}} \int_0^\infty d\omega \left[\vec{E}^+(\vec{r}, \omega) e^{-i\omega t} + \vec{E}^-(\vec{r}, \omega) e^{+i\omega t} \right] \qquad (3.10)$$

where $\vec{E}^+$ and $\vec{E}^-$ are the so called creation and annihilation operators. After substituting (3.10) into (3.9) and using the property of conjugation of those operators we obtain:

$$\Gamma = \frac{1}{\hbar^2} \sum_f \int_0^\infty d\omega \int_0^\infty d\omega' \left\langle 0 \left| \vec{\mu} \vec{E}^+(\vec{r}_0, \omega) \right| f \right\rangle$$
$$\times \left\langle f \left| \vec{\mu} \vec{E}^-(\vec{r}_0, \omega) \right| 0 \right\rangle e^{-i(\omega - \omega')t} \delta(\omega_f - \omega_0) \qquad (3.11)$$

The electric field operator includes sums over the annihilation and creation operators of all mode of the electromagnetic field, whose frequencies ω and ω' must be equal to ω_f. The summation over final states in (3.11) is therefore redundant and its removal gives

$$\Gamma = \frac{1}{\hbar^2} \int_0^\infty d\omega \int_0^\infty d\omega' \mu_\alpha \left\langle 0 \left| \hat{E}_\alpha^+(\vec{r}_0, \omega) \hat{E}_\beta^-(\vec{r}_0, \omega) \right| 0 \right\rangle$$
$$\times \mu_\beta e^{-i(\omega - \omega')t} \delta(\omega - \omega_0) \qquad (3.12)$$

where repeated subscript indices are summed over and represent Cartesian coordinates $\alpha, \beta = x, y, z$. Using fluctuation dissipation theorem and taking advantage of zero

scalar potential gauge, field correlation function may be written in the form [16]:

$$\left\langle 0 \left| \hat{E}_\alpha^+(\vec{r}_0, \omega) \hat{E}_\beta^-(\vec{r}_0, \omega) \right| 0 \right\rangle =$$
$$2\hbar\omega^2 \operatorname{Im} G_{\alpha\beta}(\vec{r}, \vec{r}', \omega) \delta(\omega - \omega') \qquad (3.13)$$

Thus decay rate expression (3.12) may be simplified

$$\Gamma = \frac{2}{\hbar} \omega^2 \operatorname{Im}[\vec{\mu} \cdot \hat{G}(\vec{r}_0, \vec{r}_0, \omega_0) \cdot \vec{\mu}] \qquad (3.14)$$

It is more convenient to use dimensionless vector potential Green function $g_{\alpha\beta}(\vec{r}, \vec{r}', \omega)$, defined as

$$\hat{G}_{\alpha\beta}(\vec{r}, \vec{r}', \omega) = \frac{\omega}{4\pi\varepsilon_0 c^3} \hat{g}_{\alpha\beta}(\vec{r}, \vec{r}', \omega) \qquad (3.15)$$

where ε_0 is the permittivity of free space. Using Eq. (3.15), the decay rate (3.14) can be rewritten in the form

$$\Gamma_\alpha = \frac{3}{2} \Gamma_0 \operatorname{Im} g_{\alpha\alpha}(r_0, r_0, \omega_0) \qquad (3.16)$$

where $\Gamma_0 = \mu^2 \omega_0^3 / 3\pi\varepsilon_0 c^3 \hbar$ is the decay rate of excited atom in free space, α defines the orientation of the dipole moment.

The electromagnetic field operators are governed by the Maxwell's equations which in the frequency domain in free space are of the form

$$\nabla \times \hat{\vec{E}}^+(\vec{r}, \omega) = i\omega \hat{\vec{B}}^+(\vec{r}, \omega) \qquad (3.17)$$

$$\nabla \times \hat{\vec{B}}^+(\vec{r}, \omega) = -i\frac{\omega}{c^2} \hat{\vec{E}}^+(\vec{r}, \omega) + \frac{1}{\varepsilon_0 c^2} \hat{\vec{J}}^+(\vec{r}, \omega) \qquad (3.18)$$

Combining Eqs. (3.12), (3.18) and (3.19) and taking into account the definition of the Fourier time transformed vector potential Green function, that is

$$\hat{\vec{A}}^+(\vec{r}, \omega) = \sum_\beta \int dr' G_{\alpha\beta}(\vec{r}, \vec{r}', \omega) \hat{\vec{J}}_\beta^+(\vec{r}, \omega) \qquad (3.19)$$

it can easily be show that

$$\sum_\mu \left(q^2 \delta_{\lambda\mu} - \frac{\partial^2}{\partial x_\lambda \partial x_\mu} + \delta_{\lambda\mu} \nabla^2 \right) G_{\mu\nu}(\vec{r}, \vec{r}', \omega) \qquad (3.20)$$
$$= -\frac{1}{\varepsilon_0 c^2} \delta_{\lambda\nu} \delta(\vec{r} - \vec{r}')$$

Thus the problem of solving of Maxwell equations is reduced to the problem of solving differential equation for Green function with appropriate boundary conditions. That is why the Green function contains information about the
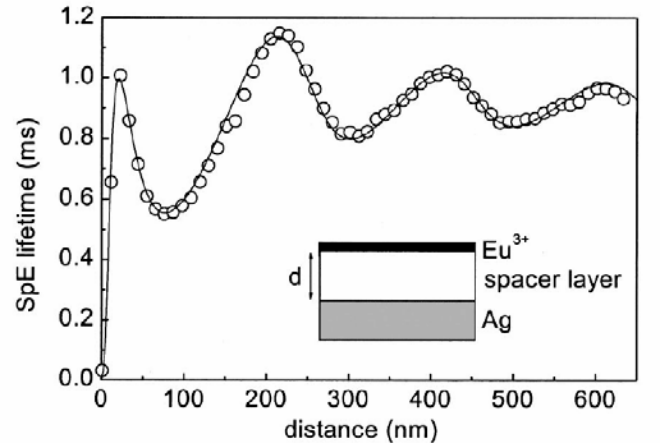

Fig.1. SpE lifetime of a monolayer of Eu^{3+} ions situated above a planar silver mirror as a function of ion-mirror separation. Solid line-theoretical plot, circles-experimental [18].

geometry of our system. The boundary conditions at the plane interface of the conductor are governed by the boundary conditions of the different components of the electromagnetic fields. The complete derivation of all components is given in [17]. The explicit form of Green function is given in Appendix A.

Regarding the symmetry of the present problem there are two different orientations for the dipole moment of the excited atom which are known as perpendicular and parallel orientations. Let us first consider the case in which the dipole moment of the excited atom is perpendicular to the surface of the mirror at $z = z_0$. This case is represented by Γ_z in our notation. After substituting (A5) into (3.16) and (A6) into (3.16) we find:

$$\Gamma_z = \Gamma_0 \left\{ 1 - 3 \left[\frac{\cos(2q_0 z_0)}{(2q_0 z_0)^2} - \frac{\sin(2q_0 z_0)}{(2q_0 z_0)^3} \right] \right\} \quad (3.21)$$

$$\Gamma_x = \Gamma_0 \left\{ 1 - \frac{3}{2} \left[\frac{\sin(2q_0 z_0)}{2q_0 z_0} + \frac{\cos(2q_0 z_0)}{(2q_0 z_0)^2} - \frac{\sin(2q_0 z_0)}{(2q_0 z_0)^3} \right] \right\} \quad (3.22)$$

We see that in the limit $z_0 \to 0$ the decay rate tends to $\Gamma_z = 2\Gamma_0$. This is due to the fact that the image dipole is in phase with its image dipole moment. From analogous considerations x component of decay rate tends to zero when $z_0 \to 0$ (See Fig. 1). By comparing (3.8) and (3.22), we can see that both classical and quantum theory give the same results.

3.3 Coupling of excited molecule to surface plasmons

When the frequency of excited molecule transition is close to frequency of free electron density excitations or so called plasmons excited molecule starts to "feel" it more then its own image dipole. This contribute to a new dominant decay channel for the excited molecule by converting localized electronic energy into surface charge-density waves in the two-dimensional metal dielectric interface.

Theoretically this problem can be treated within the framework of Green function approach as in the previous section but now we have to take into account dispersion relation for charge density waves in metal. Fig.2 shows a couple of photon-plasmon system dispersion curves. The reflected field arises from the metal surface response to the initially emitted field. In contrast to the standing-wave boundary conditions for the perfect reflector (pure image theory) the surface charge-density waves arrange themselves in such a way as to screen the external field inside the metal
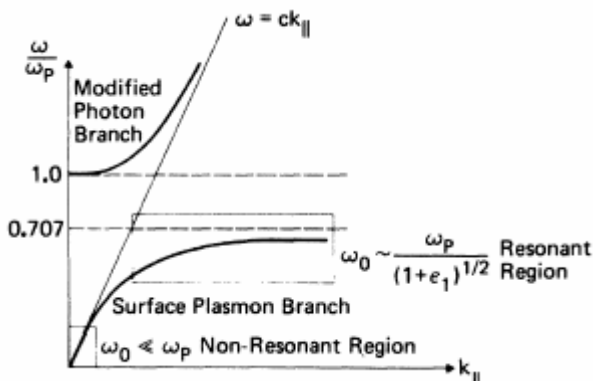
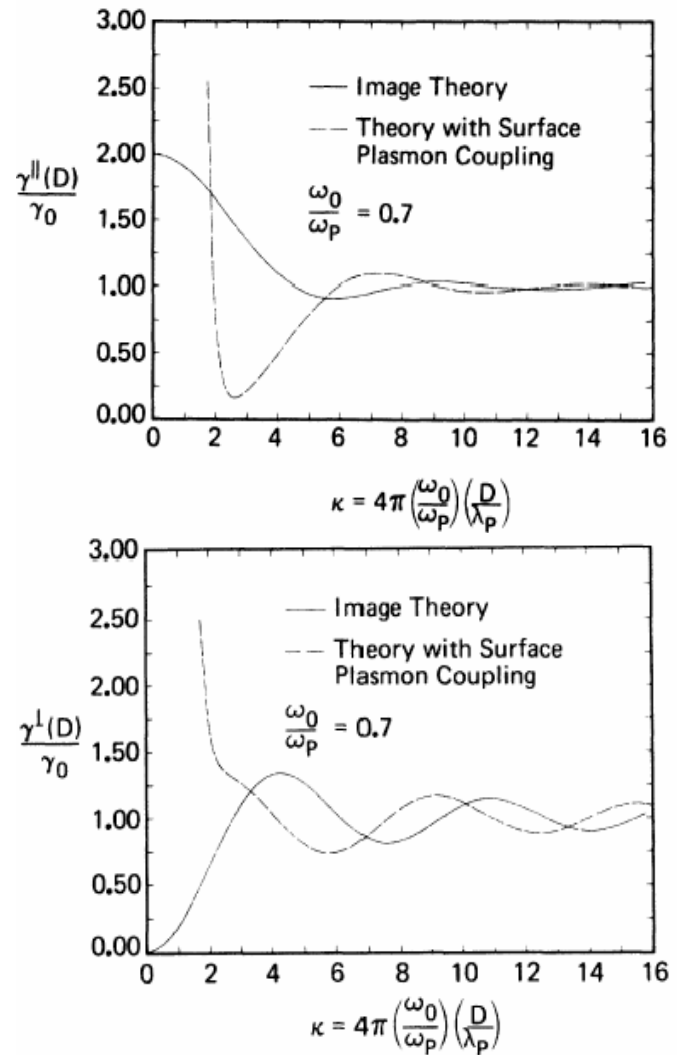Fig.2. Coupled two dimensional photon-surface plasmon dispersion curve [12]

Fig.3. Normalized decay rate $\gamma(D)/\gamma_0$ plotted as a function of phase delay near the surface plasmon resonance $\omega_0 / \omega_p = 0.7$ [12].

and set up a reflected field. The molecule evolves now in the presence of the electric field of the surface-charge response and we have to calculate the time evolution of the molecular dipole in this additional field. These calculations were carried by Morawitz and Philpott in [12]. The results show that additional terms appear in expressions for decay rate (3.22) and (3.23). These terms become the dominant decay channel for short distances. In fact, both cases, parallel and perpendicular dipole orientations, lead to divergent expressions for the decay rate, in contrast to the image results (see result (3.22) and (3.23)). Fig.3 shows the dependence of the normalized decay lifetime on phase delay. It is evident that the inclusion of the coupling of the transition dipole moment to the mixed photon-surface plasmon excitations spectrum strongly modifies the image theory, which is plotted for comparison.
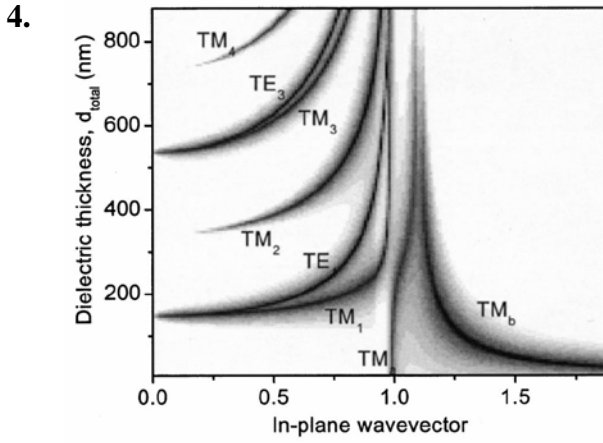
4.

Fig. 4. Calculated power dissipation function function within a metal-clad microcavity as a function of both normalized in-plane wave vector and cavity width [3]. Darker point corresponds to higher power dissipation.

Excited molecules in micro-cavities and near other nano objects

4.1. Planar microcavity

The first more complicated problem after an atom near mirror is an atom between two parallel mirrors [3]. Such a system is called an optical microcavity. Our task is as follows. As in the previous case we consider our excited atom or molecule to be a forced damped oscillator. Again it is a classical dipole which is loosing its excitation under influence of electromagnetic field reflected from cavity borders. That is why this problem is being solved straightforwardly by calculating a power dissipation function. This function depends on an in-plane wave vector $k_\parallel$. Of course it also depends on out of plane wave vector $k_\perp$, but they are related $\omega^2 = c^2(k_\perp^2 + k_\parallel^2)$. In other words calculation of power dissipation function is equivalent to calculation of radiation diagram. When power dissipation function is known decay rate is obtained by its integration $\Gamma \sim \int_0^\infty P(k_\parallel)dk_\parallel$. After integration, the following expressions for decay rate in planar microcavities were obtained [3]:

$$\Gamma_\perp = \Gamma_0\left(\frac{3\lambda}{4L}\right)\left\{1 + \sum_{n=1}^{[2L/\lambda]} 2\left[1-\left(\frac{n\lambda}{2L}\right)\right]\cos^2\left(\frac{n\pi z}{L}\right)\right\} \quad (4.1)$$

for dipole normal to the mirrors and

$$\Gamma_\parallel = \Gamma_0 \sum_{n=1}^{[2L/\lambda]} 2\left[1+\left(\frac{n\lambda}{2L}\right)\right]\sin^2\left(\frac{n\pi z}{L}\right) \quad (4.2)$$

By looking at the form of the power dissipation spectrum (Fig. 4.) we can learn much about the modes the microcavity structure. A photon may be emitted if the structure in which it is embedded supports a photonic mode at the emission frequency. There is a constructive and destructive interference of cavity modes with emitter. In terms of quantum theory the strength with which cavity supports emission is defined by photonic mode density (PMD). The larger is PMD the higher emission rate. When modes are not allowed their photonic mode density is zero and emission at their frequency is inhibited. The frequencies of these modes depend on the thickness of the microcavity,
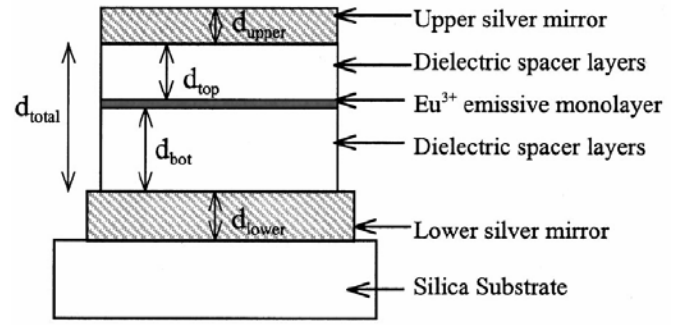
dielectric constant of the microcavity and reflection coefficients of the microcavity mirrors.

As the thickness of the cavity increases, so does the number of the allowed modes but their influence on spontaneous emission decreases. As we can see from Fig. 1., when a certain value (which is equal to half wavelength) of the cavity thickness is reached the lowest order waveguide modes appears. This and some higher order modes are split into two due to difference in reflection coefficients for TE and TM polarizations. As far as the thickness is less then half wavelength there is no waveguide modes in the cavity, instead there are SPP modes which correspond to in-plane propagation surface plasmon-polaritons in mirrors of the cavity. As we discussed in previous section coupling with these modes is particularly strong within small distances between mirrors.

To prove the validity of these calculations based on classical theory let consider an experiment that was carried out by Worthing and others in work [20]. In this work a series of microcavity samples with different and highly controlled thicknesses was made. A scheme of such microcavity is shown on Fig. 5. Emissive monolayer is placed between two dielectric layers, which in their turn are bound by two mirrors made of silver. All the system is grown up on the silica substrate.
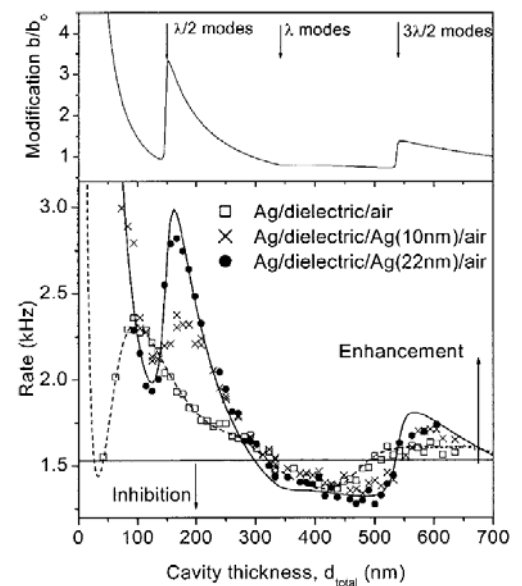

Fig. 5. Schematics of the planar microcavity

Fig. 6. Spontaneous emission rate of the Eu^{3+} monolayer as a function of the total thickness of the microcavity

6

The microcavity samples were constructed in the following way. Initially the lower silver mirror was deposited by the thermal evaporation under high vacuum onto a clean silica substrate. The thickness could be highly controlled by quartz crystal. Dielectric spacer layers were deposited with the help of Langmuir-Blodgett (LB) technique. It allowed measuring their thickness with precision of single monolayer (typically 2.5 nm thick). The emissive layer was also deposited in the same way, as a replacement of dielectric monolayer. The final step was vapor deposition of silver mirror on top on dielectric spacer layer. The thickness of that layer also could be changed allowing control of reflection coefficient. An Eu^{3+} chelate was used as the emissive monolayer due to its near monochromatic emission at λ=614 nm (linewidth ~ 4 nm) and relatively long fluorescence lifetime (~ 1 ms).

Microcavity samples were excited by a laser pulse (λ=337 nm) through semi-transparent upper mirror. By observing the time evolution of the resulting fluorescence the decay rate was determined. The results for different cavity thicknesses are shown on Fig. 6. We can clearly see decay rate enhancement as well as inhibition. In the vicinity of the peaks the thickness of the cavity is integer number of half wavelengths, thus indicating a strong coupling to cavity waveguide modes. These results are in a good agreement with previously calculated by formulae (4.1-4.2) and depicted on the upper part of the Fig. 6.

4.2. Spontaneous emission in a passive optical fiber. Cylindrical microcavity

Another example of bounded space is an optical fiber. The approach described in section 3.2 can be used for calculation of the decay rate in fiber. For this we only need to know the Green function tensor, which we can substitute in (3.16).

Schematically an optical fiber is shown in Fig. 7. It is a step-index structure with n_1 and n_2 corresponding to refractive index of the core region and cladding. The diameter of the core is $2a$ and cladding is considered to be infinite. Because of the cylindrical symmetry this system is studied in cylindrical coordinates (ρ,φ,z). The spontaneous emission of dipoles of both orientations, along z axis and perpendicular to it, were studied in work [21]. The decay rate
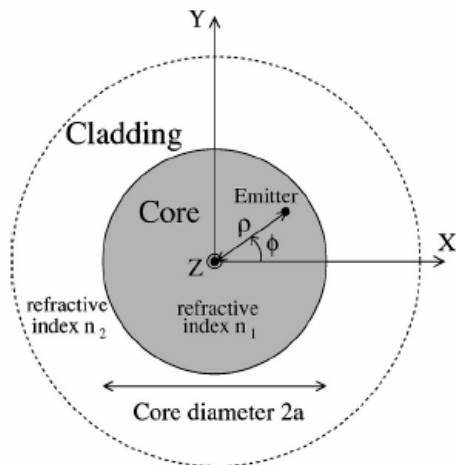

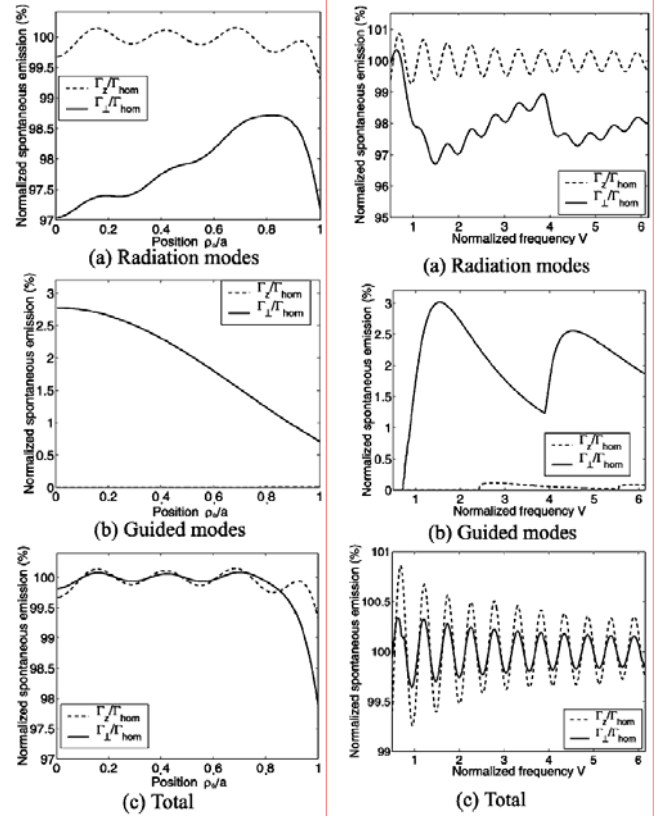Fig. 7. Optical fiber with core refractive index n_1, cladding refractive index n_2, and core diameter 2a

Fig. 8. Spontaneous emission as a function of position of an emitter in the core of a step-index fiber with n1=1.45,n2=1.43, a=2μm, λ=1560nm [21]

Fig. 9. Spontaneous emission as a function of normalized frequency for an emitter located in the center of the core of a step-index fiber with n1=1.45,n2=1.43,a=2μm[21].

is calculated as a function of the distance ρ from the fiber axis z. Taking into account the circular symmetry of the problem, the solutions of the Maxwell equations can be given in the form of cylindrical functions. It appears that eigensolutions may be divided into two types of solutions, which are called radiation and guided modes. The details of analytical derivation of an explicit Green function tensor are given in [21].

The results of distance dependant spontaneous emission rate are presented on Fig. 8. The transition wavelength of emitter is 1560 nm. The spontaneous emission into radiation mode shows quasi-periodic dependence on the distance that is the result of cavity effect due to constructive-destructive interference with electromagnetic waves reflected from core-cladding interface. Rough estimate of the period gives:

$$\frac{\Delta\rho_0}{a} \approx \frac{\lambda_0}{2an_1} \qquad (4.3)$$

After substituting all the parameters of the system in (4.3) it gives $\Delta\rho_0 \approx 0.27$. From the plot (Fig. 8. (c)) it can be seen that period varies in the range from 0.26 to 0.28.

Also we can see that spontaneous emission into guided modes is much weaker then into radiation mode. Moreover there is no emission into guided modes for the case of dipole orientation along the z axis that is due to the fact that cavity modes of the cylindrical resonator do not have component of the electric field in z direction. The total spontaneous emission rate is around spontaneous emission rate in homogeneous dielectric ($\Gamma_{hom} = \omega_0^3\mu^2 n_1 / 3\pi\hbar\varepsilon_0 c^3$),

experiencing small enhancement in some regions and small inhibition in others. Also it is clearly seen that the spontaneous emission rate for different orientations differ at the edge of the core. That is due to different boundary conditions at the core cladding interfase for each component of the electric field; the z component is constant across the interface whereas components in xy plane differ by the factor of $n_1^2 / n_2^2 = 1.03$.

On Figure 9 we can see spontaneous emission plotted as a function of normalized frequency $V = \frac{2\pi\omega_0}{c}\sqrt{n_1^2 - n_2^2}$ for the emitter placed in the center of the fiber core ($\rho_0 = 0$). Again we see oscillations in the spontaneous emission rate for radiation mode. It has the same reason, constructive-destructive interference. A frequency threshold is observed for emission into guided modes, that is in a good agreement with condition for mode propagation in such step-index optical fiber V>1. Analogous threshold is observed at V=4, but now for waveguide modes with angular momentum m=±2. As there starts emission into guided mode the spontaneous emission into radiation mode weakens what is clearly seen from plot for perpendicular component of the spontaneous emission (Fig. 9. (a)). Also we can see that there appears a weak radiation into the z component of guided modes at V≈2.4 and V≈4.8 for waves with angular momentum m=±1 and m=±2 correspondingly. That is were a single mode condition for step-index fiber does not hold and z-component of the electric field appears.

4.3. Spontaneous emission near two nano-spheres

Another interesting problem is the spontaneous emission near spherical nano particles. Specifically it is calculated for a dipole between two metallic spheres [22]. Both orientations of the dipole, parallel and perpendicular to the axis going through centres of spheres, are considered and
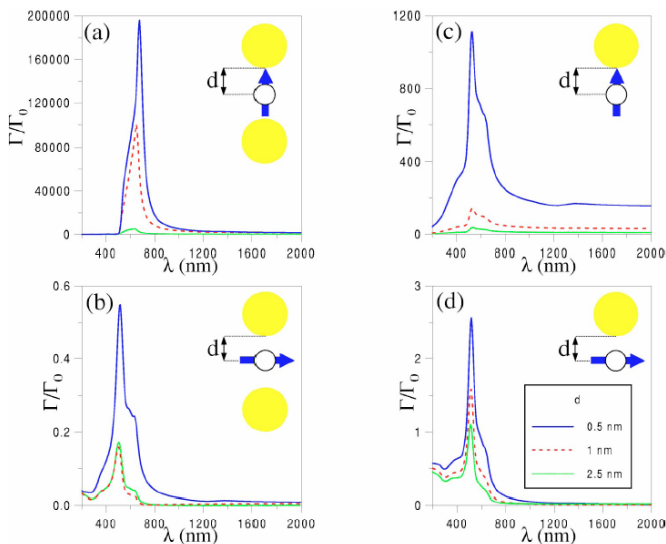
Fig. 10. (a) Spontaneous emission rate normalized to vacuum for an atom situated between two gold spheres of radius 50 nm, and with its electric dipole oriented parallel to theline that crosses the center of the spheres. Three different sphere separations are considered, so that the distance from the atom to eachof the spheres is 0.5, 1, or 2.5 nm (the rate increases with decreasing distance). (b) Same as (a) when the dipole is oriented perpendicular with respect to the one in (a). (c) (d) Same as (a) and (b), respectively, but with only one sphere [22].
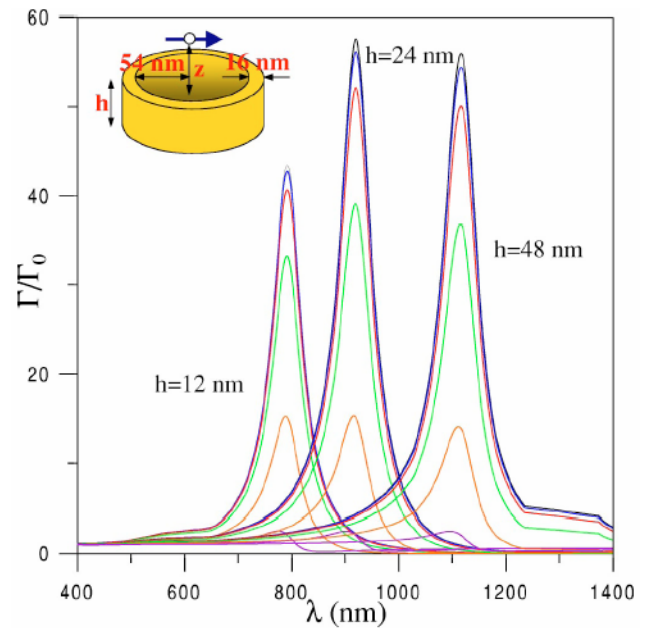
FIG. 11. Emission probability normalized to vacuum from an atom placed at the axis of a nano-ring of height h at a distance z from its center. The transition electric dipole is oriented perpendicular to the ring axis. The three peaks correspond to different values of h. Within each peak, the values of z are (from the top to the bottom) 0, 6, 12, 24, 48, and 96 nm, respectively [22].

in both case strong enhancement of spontaneous emission within certain range of frequencies is observed (Fig. 10.). That can be explained by the fact that dipole is placed very close to the spheres (~1nm) and it starts to interact with surface plasmons. Indeed the frequency region of the enhancement corresponds to the plasma frequency of the material. We can see that there is very strong enhancement in spontaneous emission rate for the case of emitter dipole being parallel to axis, whereas in perpendicular case an inhibition is observed (although not so strong for plasma resonance region). This is due to the image dipole cancelling or doubling the real one, as in the case of the emission near the plane mirror. It can also be seen that both the enhancement and the position of the maximum depend on the distance between spheres. The enhancement decreases with distance increase and the maximum position is slightly shifted to the higher frequencies. It should be noted that for the case of one sphere (Fir. 10. (c)) the enhancement is not so strong, as well as the inhibition it the case of perpendicular to the axis dipole (Fir. 10. (d))

4.4. Emission near gold nano-ring

In the same work [22] the spontaneous emission near golden nano-ring is studied. This kind of nano-rings is known for their properties to show infrared plasmon resonances in the extinction part of the spectrum, which is a particular result of their shape. Solid discs do not have such a property. In [22], the atom was placed on the ring axis at several distances from the center of the ring and the probability of emission related to the case in which there is only vacuum surrounding the atom was calculated. Results are shown in Fig. 11.

There is no considerable enhancement in the emission rate when the dipole is oriented parallel to the ring axis, that is why the results for this case are not presented

here. For the perpendicular orientation of the dipole a strong amplification of the emission rate is observed which also depends on the distance between the emitter and the centre of the ring z. The maximum enhancement occurs when the atom is in the centre of the ring, decreasing with the distance z increase, but still considerable even when the atom is above the ring. The position of the maxima grows with the height of the ring.

4.5. Experimental measurement of spontaneous emission near spherical nanoparticle

To prove validity of the theory very interesting experiment was carried out [23]. An influence of spherical particle on fluorescence of single molecules was studied. For that a solution with emitter molecules (in this case molecules of the nile blue) was placed on the cleaned thin glass plate. To fix position of the molecules the sample was overcoated with thin layer of polymethyl methacrylate (PMMA). The thickness of PMMA layer, which is needed for theoretical calculation, could be readily defined by razor-blade scratching with subsequent atomic force microscopy (AFR) measurements. After spin coating, molecules of nile blue were randomly orientated. To determine their orientation an position a raster scanning of the layer with emitters was carried by focusing laser onto the surface of the sample (wavelength λ=637 nm). By analyzing recorded fluorescence rate pattern in is possible to find position of molecules with dipole moment perpendicular to the surface. The investigation of these molecules with spherical particles is further investigated.

A spherical golden particle with diameter d=80 are attached to the end of a pointed optical fiber as shown by the SEM image on the inset of Fig. 12(a). A constant distance z between surface and fiber was maintained by attaching to it tuning-fork crystal resonant frequency depends on z and serves as a feedback loop.

The results for the spontaneous emission rate for molecules with vertical orientation of the dipole moments are depicted on Fig.12(a). The fluorescence rate increases with decrease of the particle surface separation and reach the maximum value at z≈5 nm. For shorter distances quenching
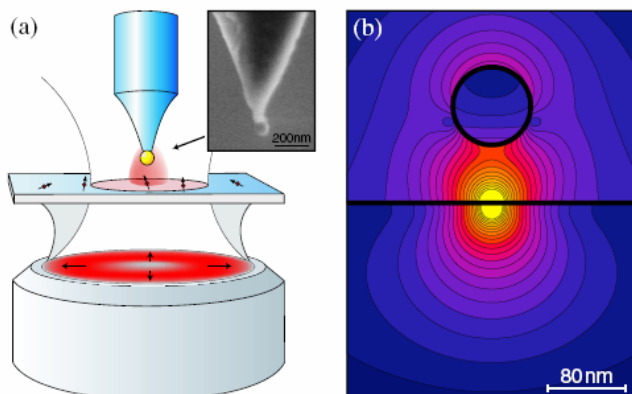

Fig.12. (a) Sketch of experimental arrangement. Inset: SEM image of a gold particle attached to the end of pointed optical fiber. (b) Field distribution of an emitting dipole (λ=650 nm) located 2 nm underneath the surface of a glass substrate and faced by gold particle separated by a distance of z=60 nm from the glass surface [23].
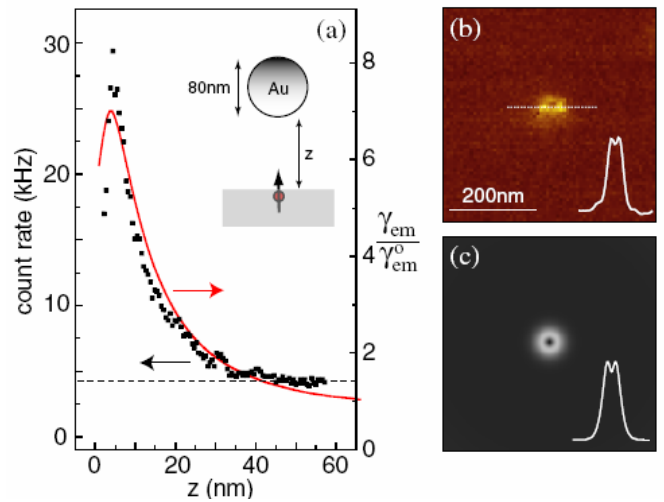

Fig. 13. (a) Fluorescence rate as a function of particle-surface separation z for a vertically oriented molecule (solid curve: theory, dots: experiment). The horizontal dashed line indicates the background level. (b) Fluorescence rate image of a single molecule acquired for z=2 nm. The dip in the center indicates fluorescence quenching. (c) Corresponding theoretical image[23].

in spontaneous emission is observed. Experimental data (dots on the plot) show good agreement with theoretical calculations in high rate region. There is disagreement in the law rate region that is due to high background noise of gold luminescence. Other sources of noise are calibration tolerances and the fact that dipole is not strictly perpendicular to the surface. A typical fluorescence rate pattern for vertically oriented molecule is depicted on Fig. 13(b,c). By looking at such kind of fluorescence distribution it was possible to determine the orientation of the molecules

5. Fluorescence in Photonic Crystals

Photonic crystals (PC) have been the subject of intensive research over the past two decades since their proposal by Yablonovich [8]. Photonic crystals are one-, two- or three-dimensional artificially designed periodic structures with a period of the order of light wavelength. Because of their ability of Bragg scattering, a band structure for photon propagation may be forms. The propagation of light in such structures is vary similar to propagation of electrons is conventional crystals. By varying materials and periodicity of photonic crystal, the photonic dispersion relation and thus the electromagnetic mode structure of a PC can be altered, that can be used in variety of devices. The most interesting modification of the photon dispersion occurs when the linear propagation of a photon in a PC is prohibited in all directions for a range of frequencies, thus creating a complete photonic band gap (PBG).

The radiative dynamics of an optically active material placed within or near a PC can be dramatically modified from that of free space. This is a result of the ''colored'' electromagnetic reservoir provided by the solutions to the electromagnetic field equations within a PC. In the optical domain, theoretical studies of atomic transitions coupled to the EM modes of a PC with an optical PBG predict a number of novel quantum optical phenomena. These phenomena include the suppression or enhancement of spontaneous emission and the associated fractional localization of light near radiating atoms [25]; rapid all-optical switching [26]; and anomalous superradiant emission,

as well as low-threshold lasing near the edge of a PBG [27]. A manufacturing of photonic crystals is still not easy task, that is why their optical properties must be calculated before making them. In this section of the paper a method of calculation of spontaneous emission will be presented and applied to some real systems.

5.1. Equation of motion for spontaneous emission

Let us consider a two level atom which is emitting in the photonic crystal. To calculate spontaneous emission rate we again have to consider a system atom-radiation field. Suppose we know the wave function of such a system for certain moment in time:

$$|\psi\rangle = b_2(\vec{d}, \vec{r}_0, t)|2, \{0\}\rangle + \sum_\mu b_{1,\mu}(\vec{d}, \vec{r}_0, t)|1, \{\mu\}\rangle e^{-i\Delta_\mu t} \quad (5.1)$$

That is a superposition of quantum state, where $|2, \{0\}\rangle$ is an excited state of atom and $|1, \{\mu\}\rangle$ is one of possible photonic stated, μ defines direction of emitted photon; $\Delta_\mu = \omega_\mu - \omega_{21}$. $b_2(\vec{d}, \vec{r}_0, t)$ and $b_{1,\mu}(\vec{d}, \vec{r}_0, t)$ denote the probability of the atom staying in excited state or emitting a photon in one of the photonic states accordingly. To find spontaneous emission rate we have to know how $b_2(\vec{d}, \vec{r}_0, t)$ is changing in time. For that we need to know a total Hamiltonian of the system.

The Hamiltonian for the charged particle in electromagnetic field is:

$$H_{el} = \frac{1}{m_e}[\vec{p} - e\vec{A}(\vec{r})]^2 - e\Phi(\vec{r}) \quad (5.2)$$

This problem is more conveniently solved under the gauge in which scalar potential vanishes. In quantum electrodynamics there is a common procedure of quantization of the field operator that is expanding it via annihilation and creation operators which commute among each other. By doing this and using a property of periodicity of the field (mode functions may be presented in the basis of Bloch modes) an expression for the Hamiltonian was obtained in [28]:

$$H_{tot} = \frac{\hbar}{2}\omega_{21}\sigma_z + \hbar\sum_\mu \omega_\mu a_\mu^\dagger a_\mu + i\hbar\sum_\mu (g_\mu a_\mu^\dagger \sigma_- - g_\mu^* \sigma_+ a_\mu) \quad (5.3)$$

where μ denotes the energy band and wave vector of a given field mode. $a_\mu^\dagger$ and a_μ are the creation and annihilation operators, a_μ (j=+,−) are the Pauli operators. Also atom-field mode coupling constant is given by the formula:

$$g_\mu(\vec{d}, \vec{r}_0) \equiv g_\mu = \omega_{21}d_{21}\sqrt{\frac{1}{2\hbar\varepsilon_0\omega_\mu V}}\vec{d}\vec{E}_\mu^*(\vec{r}_0) \quad (5.4)$$

By substituting Hamiltonian (5.3) and wave function (5.1) into nonstationary Schrodinger equation we obtain so called equations of motion for probabilities:

$$\frac{d}{dt}b_2(\vec{d}, \vec{r}_0, t) = -\sum_\mu g_\mu b_{1,\mu}(\vec{d}, \vec{r}_0, t)e^{-i\Delta_\mu t} \quad (5.5)$$

$$\frac{d}{dt}b_{1,\mu}(\vec{d}, \vec{r}_0, t) = g_\mu b_2(\vec{d}, \vec{r}_0, t)e^{i\Delta_\mu t} \quad (5.6)$$

After integrating Eq. (5.6) and substituting the result into (5.5) we obtain an equation for excited the state amplitude:

$$\frac{d}{dt}b_2(\vec{d}, \vec{r}_0, t) = -\int_0^t G(\vec{d}, \vec{r}_0, t - t')b_2(\vec{d}, \vec{r}_0, t)dt' \quad (5.7)$$

which is expressed via time delay Green function

$$G(\vec{d}, \vec{r}_0, \tau) \equiv \theta(\tau)\sum_\mu \left|g_\mu(\vec{d}, \vec{r})\right|^2 e^{-i\Delta_\mu t} \quad (5.8)$$

It describes an influence of the electromagnetic vacuum on the atoms, containing information not only about present state of the system but also about the past. From the causality considerations this function should vanish for $\tau<0$, than is why Heaviside step function is included as a pre-factor in (5.8).

After substituting (5.4) into (5.8), and making explicit summation over wave-vectors (integration over the band) we get:

$$G(\vec{d}, \vec{r}_0, \tau) = \theta(\tau)\alpha\sum_n \int_{1BZ} d\vec{k}\frac{e^{-i\Delta_{n,\vec{k}}\tau}}{\omega_{n,\vec{k}}}\left|\vec{d}\cdot\vec{E}_{n,\vec{k}}(\vec{r}_0)\right|^2 \quad (5.9)$$

where integration is over the first Brillouin zone. If we add to (5.9) one more frequency integration over delta function the result will not change:

$$G(\vec{d}, \vec{r}_0, \tau) = \theta(\tau)\alpha\sum_n \int_0^\infty d\omega\frac{e^{-i(\omega-\omega_{21})\tau}}{\omega}$$
$$\times\int_{1BZ} d\vec{k}\delta(\omega - \omega_{n,\vec{k}})\left|\vec{d}\cdot\vec{E}_{n,\vec{k}}(\vec{r}_0)\right|^2 \quad (5.10)$$

Now we can introduce a projected density of states (PDOS) that is not to be confused with density of states (DOS) which counts a number of modes at a given frequency:

$$N_p(\vec{d}, \vec{r}_0, \omega) = \sum_n \int_{1BZ} d\vec{k}\delta(\omega - \omega_{n,\vec{k}})\left|\vec{d}\cdot\vec{E}_{n,\vec{k}}(\vec{r}_0)\right|^2 \quad (5.11)$$

PDOS is a number of modes available at a given frequency for particular orientation and position of the atom. In order to calculate spontaneous emission rate we have to know average emission characteristics for all orientations of atoms. For that we have to make orientational average of the time delay Green function:

$$G_f(\tau) \equiv \left\langle G(\vec{d}, \vec{r}_0, \tau)\right\rangle_{r,\theta}$$
$$= \theta(\tau)\beta\int_{WSC} d\vec{r}\frac{\rho(\vec{r})}{N_e}\int_0^\infty d\omega\frac{N_l(\vec{r}, \omega)}{\omega}e^{-i(\omega-\omega_{21})\tau} \quad (5.12)$$

where integration over $\vec{r}$ is carried out within Wigner-Seitz cell of photonic crystal. In (5.12) we have introduced a distribution function of emitters $\rho(\vec{r})$ and local density of states (LDOS), which is an orientational average of the PDOS.

$$N_l(\vec{r}, \omega) \equiv \frac{3}{4\pi}\left\langle N_p(\vec{d}, \vec{r}_0, \omega)\right\rangle_\theta$$
$$= \sum_n \int_{1BZ} d\vec{k}\delta(\omega - \omega_{n,\vec{k}})\left|\vec{E}_{n,\vec{k}}(\vec{r}_0)\right|^2 \quad (5.13)$$

The replacement $G(\vec{d}, \vec{r}_0, \tau)$ in by $G_f(\tau)$ (5.7) gives the equation of motion for the probability amplitude of the excited state population in spontaneous emission. As the averaging in (5.7) should be done from both sides of the equality sign we will denote the average probability by $b_f(\tau)$ and the final equation of motion is:

$$\frac{d}{dt}b_f(t) = -\int_0^t G_f(t-t')b_f(t')dt' \quad (5.14)$$

As we can see from (5.13) spontaneous emission rate is completely determined by the time delay which in its turn is determined by local density of states of the photonic crystal. In nets section we will consider results of the calculation of LDOS for real system.
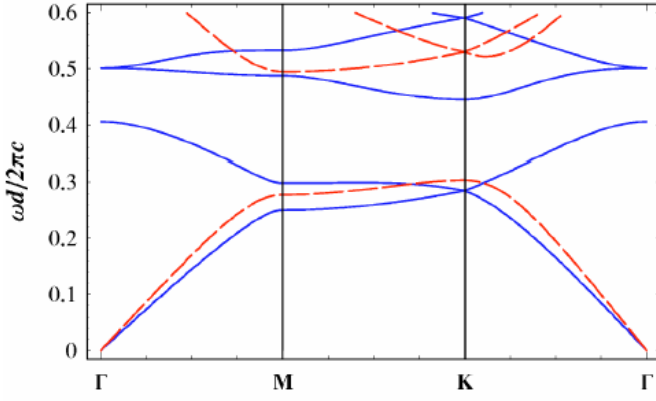
FIG. 13. 2D band structure for a hexagonal (or triangular) array of air-voids in a dielectric. The array parameters are $a_l / d = 0.45$, $n_l = 1.0$ and $n_b = 3.4$ The TM modes are shown as solid lines and the TE modes are shown as dashed lines [29].

5.2. Local density of States in real photonic systems. Porous Silicon Clusters

In this section we will consider LDOS in a hexagonal cluster of cylindrical air-voids in a dielectric background [29]. Although macroporous silicon can be manufactured within a broad range of air-void radius we will consider here an air-voids with radius $a_l / d = 0.45$ (d period of 2D PC) because is was found to give the most interesting results. The main emphasis is on macroporous silicon with a silicon background of refractive inde $n_b = 3.4$. The inplane band structure for such two dimensional periodic structure is shown in Fig. 13. TE gaps are favored in this type of 2D PC, and it has a wide TE-gap in the frequency (normalized) range $\omega d / 2\pi c = 0.303 - 0.495$. There is also a narrower gap for TM modes in the frequency range $\omega d / 2\pi c = 0.405 - 0.445$. This gap fully lies within TE-gap, thus creating a complete photonic band-gap.

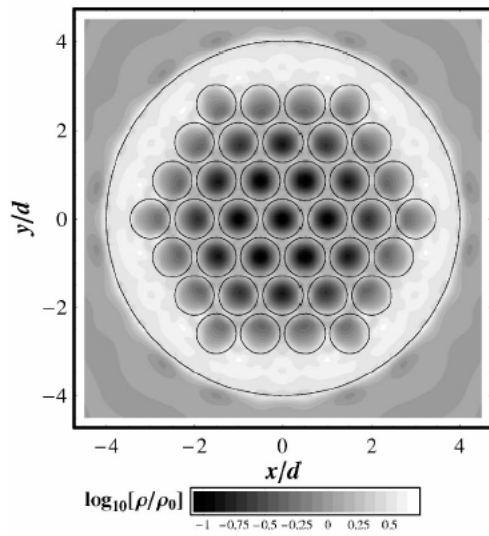Initially a 3D local density of states in macroporous

FIG. 15. 3D LDOS across the plane of a macroporous silicon cluster enclosed by an air-jacket. The frequency is $\omega d / 2\pi c = 0.449$ and the cluster parameters are N_c=37, $a_l / d = 0.45$, $n_l = 1.0$, $n_b = 3.4$ and $a_0 / d = 4.0$. The 3D LDOS is normalized to its freespace value, $\rho_0 = \omega^2 / \pi^2 c^3$ [29].
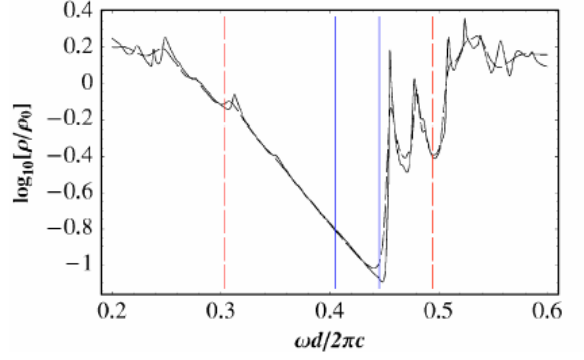

FIG. 16. 3D LDOS vs frequency in macroporous silicon at $(x, y) = (0,0)$ (in the center of cluster) with an air-jacket (solid line) and without (dashed line). The inner pair of vertical lines indicates the edges of the in-plane TM gap and the outer pair indicates the edges of the TE [29].

silicon was studied for a cluster of air-voids in an infinite silicon background (without an air jacket) [30]. In Fig. 15, the 2D cut of a 3D LDOS is shown across the perpendicular to air-voids plane of a macroporous silicon cluster enclosed by an air-jacket. The cluster consists of 37 hexagonally packed air-voids that are covered by cylindrical air jacket of the radius $a_0 / d = 4.0$. The radiation frequency is chosen to be just below the top of the complete band gap $\omega d / 2\pi c = 0.445$, strongly suppressing the emission if it was a bulk porous silicon. The local density of stated is the lowest in the center of the cluster gradually increasing to outer air-voids hexagon. That is in agreement with the fact than in the center of the cluster the porous silicon has more bulk properties. Outside the cluster in the jacket the LDOS acquires its free space value.

Figure 16 shows a 3D LDOS at the center of the cluster as a function of normalized frequency. The results are compared with those of an infinite silicon background and show that the effect of air jacket is small that is the maximum suppression of the LDOS is slightly bigger for the case with jacket. The LDOS show quite sharp step in frequency domain while crossing the top of the complete band gap. There is also quite big step near top of the band gap for the TE modes. From the bottom side of the gap we can observe gradual change in the LDOS with the frequency.

Conclusions

In the present paper we overviewed spontaneous emission of excited systems located in different environments.

In chapter 2, spontaneous emission is considered from a statistical point of view as one of the processes which can occur with systems with discrete energy levels (apart from stimulated emission and absorption). Furthermore, that chapter describes a physical phenomenon which lies at the heart of spontaneous emission, coupling of electromagnetic vacuum fluctuations to the excited atom and gives a scheme of calculation for the probability of spontaneous downward transitions.

As it becomes clear from chapter 3, the spontaneous emission may be strongly modified when there is a boundary, specifically the metallic mirror. It appears that the problem of SpE near the mirror can be very well described classically. The atom is considered as the classical oscillator, which

11

decays as if it was in vacuum until it feels the reflection from the mirror, which can amplify or inhibit its decay depending on the phase of the reflected wave. Experimental data are presented which are in very good agreement with theory. Furthermore this chapter describes the quantum approach to solving the problem of SpE near the boundary and shows that the decay rate can be expressed in terms of the Green function tensor, which is a solution of the Maxwell equations with certain boundary conditions and thus contains information about the environment.

When the excited molecule is quite close to the surface and the transition frequency is close to the plasma frequency, then there is strong coupling between molecule and surface plasmons that leads to a rapid increase of the decay rate due to pumping of excitation energy of molecule to surface plasmons. It gives another method of excitation of surface plasmons, which cannot be excited simply by laser beam.

Chapter 4 gives a general classical scheme of calculating SpE rate in optical microcavities and gives results for planar and cylindrical microcavities. Also SpE near nanospheres and nanorings was considered and showed good agreement with experiment.

Quite a solid theory of fluorescence in photonic crystal is presented in chapter 5. SpE is considered within a formalism of Schrödinger's equation in which the wave function contains both energy states of the atom and the quantized electromagnetic field. The Hamiltonian of atom-field interaction is also derived. It is shown that fluorescence dynamics fully depends on fluorescence Green function (5.20), which in its turn is defined by local density of states. LDOS is a number of modes in unit frequency interval at a certain point. It depends on the position of the atom and may be strongly suppressed within a band gap frequency range. It means that if the transition frequency of the atom is within the band gap of PC the spontaneous emission will be inhibited. The results of theoretical calculation of LDOS porous silicon are presented in the end of the chapter.

Spontaneous emission in PC is not only important from the point of view of applications in optoelectronic devices but also from the point of view of research. It can help in the study of the LDOS within band gap region, which is not accessible for light because of non-propagation.

Appendix A

The explicit form of the coordinate space Green function for the system with an ideal mirror can be written as [15]

$$G_{\alpha\beta}(\vec{r},\vec{r}',\omega) = G'_{\alpha\beta}(\vec{r},\vec{r}_0',\omega) \pm G'_{\alpha\beta}(\vec{r},\vec{r}_1',\omega)$$
$$-\frac{1}{3\varepsilon_0\omega^2}\delta_{\alpha\beta}\delta(\vec{r}-\vec{r}') \qquad (A1)$$

where the plus sign holds for $\alpha\beta = xy, yz, zz$ and minus sign holds for the other components. The tensor $G'_{\alpha\beta}(\vec{r},\vec{r}_i',\omega)$ is given by

$$G'_{\alpha\beta}(\vec{r},\vec{r}_i',\omega) = \frac{q^3}{4\pi\varepsilon_0\omega^2}\left\{\left(\frac{1}{qr_{rel}}+\frac{1}{(qr_{rel})^2}-\frac{1}{(qr_{rel})^3}\right)\delta_{\alpha\beta}\right. \qquad (A2)$$
$$\left.-\left(\frac{1}{qr_{rel}}+\frac{2i}{(qr_{rel})^2}-\frac{3}{(qr_{rel})^3}\right)\frac{(\vec{r}_{rel}\vec{r}_{rel})_{\alpha\beta}}{(r_{rel})^2}\right\}e^{iqr_{rel}}$$

where $\vec{r}_{rel}\vec{r}_{rel}$ is the normal Cartesian dyadic tensor and

$$\vec{r}_{rel} = \vec{r} - \vec{r}_i, \ i = 0,1 \qquad (A3)$$

The vectors $\vec{r}_i$ are defined as

$$\vec{r}_0 = \vec{r}', \vec{r}_1' = \vec{r}' - 2z'k \qquad (A4)$$

The typical structure of a semi-infinite response function is seen in Eq. (A1). The bulk part, which is the first term together with the delta function term, is associated with direct communication between the two points $\vec{r}$ and $\vec{r}'$ and resembles a free space Green function. The second term displays the communication between the points via a reflection in the perfect conducting interface. This term corresponds to the so called image source.

From (A2) we can derive explicit form of some components which are used in main text of this paper. Taking into account (16):

$$g_{zz}(\vec{r}_0,\vec{r}_0,\omega_0) = \frac{2}{3}i - 2\left(\frac{i}{(2q_0z_0)^2}-\frac{1}{(2q_0z_0)^3}\right)e^{2iq_0z_0} \ (A5)$$

$$g_{xx}(\vec{r}_0,\vec{r}_0,\omega_0) = \frac{2}{3}i - \left(\frac{1}{2q_0z_0}+\frac{i}{(2q_0z_0)^2}-\frac{1}{(2q_0z_0)^3}\right)e^{2iq_0z_0} \ (A6)$$

where z_0 distance from atom to the surface of the mirror, $q_0 = \omega_0/c$.

References
[1] E. M. Purcell, Phys. Rev. **69**, 681 (1946)
[2] P. W. Milonni et al., Opt. Commun. **9**, 119 (1973)
[3] Jeong-Ki Hwang, Phys. Rev. B **60**, 4688 (1999)
[4] F. de Martini et al., Phys. Rev. Lett. **59**, 2955
[5] F. de Martini et al., Phys. Rev. A **43**, 2480 (1991)
[6] E. Snoeks et al., Phys. Rev. Lett. **74**, 2459 (1995)
[7] E. Yablonovitch et al., Phys. Rev. Lett. **61**, 2546 (1988)
[8] E. Yablonovitch, Phys. Rev. Lett. **58**, 2059 (1987)
[9] M. Florescu et al., Phys. Rev. A, **64**, 033801 (2001)
[10] K. H. Drexhage , J. Luminescence **1,2** (1970) 693-701
[11] I. Pockrand, A. Brillante, Chem. Phys. Lett. **69**, 499 (1980)
[12] H. Morawitz, M. R. Philpott, Phys. Rev. B **10**, 4863 (1974)
[13] M. R. Philpott, J. Chem. Phys. **62**, 1812 (1975)
[14] H. Kuhn, J. Chem. Phys. **53**, 101 (1970)
[15] R. Matloob, Phys. Rev. A **60**, 3421 (1999)
[16] L. Landau and E. Lifshits, *Statistical Physics*, (Pergamon, Oxford, 1980), Part 2.
[17] R. Matloob, Phys. Rev. A **62**, 022113 (2000)
[18] P. Andrew et al., Phys. Rev. B **64**, 125405 (2001)
[19] Rignealut, et al., Phys Rev. A, **55**, 1497 (1997)
[20] P. T. Worthing et al., J. Appl. Phys. **89**, 615 (2001)
[21] T. Sondergaard et al., Phys. Rev. A, **64**, 033812 (2001)
[22] L. Blanco et al., Phys. Rev. B **69**, 205414 (2004)
[23] P. Anger, P. Bharadwaj, L. Novotny, Phys. Rev. Lett. **96**, 113002 (2006)
[24] L. Novotny et al., Phys. Rev. Lett. **86**, 5251 (2001)
[25] S. John et al., Phys. Rev. Lett. **64**, 2418 (1990)
[26] S. John et al., Phys. Rev. Lett. **78**, 1888 (1997)
[27] N. Vats et al., Phys. Rev. A **58**, 4168 (1998)
[28] N. Vats et al., Phys. Rev. A **65**, 043808 (2002)
[29] D. P. Fussell et al., Phys. Rev. E **70**, 066608 (2004)
[30] D. P. Fussell et al., Phys. Rev. E **67**, 045601 (2003)